Materials Today Bio 16 (2022) 100410

Contents lists available at ScienceDirect

Materials Today Bio

journal homepage: www.journals.elsevier.com/materials-today-bio

The endothelium permeability after bioresorbable scaffolds implantation caused by the heterogeneous expression of tight junction proteins

Junyang Huang, Shuang Ge, Desha Luo, Ruolin Du, Yang Wang, Wanling Liu, Guixue Wang **, Tieying Yin *

Key Laboratory for Biorheological Science and Technology of Ministry of Education, State and Local Joint Engineering Laboratory for Vascular Implants, Bioengineering College of Chongqing University, Chongqing, 400030, China

ARTICLE INFO

Keywords:
Bioresorbable scaffolds (BRSs)
Poly-*l*-lactic acid (PLLA)
Tight junction proteins (TJPs)
Endothelium permeability
Mechanical stimulation

ABSTRACT

As one of the main functions of vascular endothelial cells, Vascular permeability is determined by four tight junction proteins (TJPs): Zonula Occludens-1 (ZO-1), Claudin-5, Occludin and Tricellulin. The barrier function of blood vessels will be reconstructed after they are damaged by endothelial mechanical injuries caused by vascular interventions. In this study, the effects of balloon expansion (transient mechanical injury) on four TJPs and vascular permeability were compared with those of poly-*l*-lactic acid bioresorbable scaffolds (BRSs) implantation (continuous mechanical stimulation). We found that BRSs do not affect vascular permeability, while the recovery of vascular barrier function was found to be only related to the mechanical injuries and repair of endothelium. Mechanical stimulation affects and accelerates the recovery process of vascular permeability with the heterogeneous expression levels of TJPs induced after BRSs implantation. Different TJPs have different sensitivity to different loyal mechanical stimuli. ZO-1 is more sensitive to shear stress and tension than to static pressure. Occludin is sensitive to static pressure and shear stress. Tricellulin is more sensitive to tension stretching. Compared with the other three TJPs, Claudin-5 can respond to mechanical stimulation, with relatively low sensitivity, though. This difference in sensitivity determines the heterogeneous expression of TJPs. Mechanical stimulation of different kinds and strengths can also cause different cell morphological changes and inflammatory reactions. As an important element affecting endothelial function, the mechanical factors emerging after BRSs implantation are worthy of more attention.

1. Introduction

Cardiovascular diseases(CVD)s are among the most common diseases that give rise to disability and mortality [1]. Percutaneous coronary intervention with stenting has become the most effective method for treating those diseases [2,3]. Vascular stents have experienced the development from bare metal stents to bioresorbable scaffolds (BRSs), and poly-*L*-lactic acid (PLLA) is one of the most important and widely used material [4]. Vascular damage, together with a risk of thrombosis and restenosis, will inevitably be the result of stent implantation. All these things are closely related to the function of endothelial cells (ECs) [5]. Therefore, the recovery of endothelial function after stent implantation plays a key role in conducting interventional treatment.

In the vascular environment, ECs is mainly subjected to three kinds of mechanical stimulation: shear stress, tension (circumferential strain/stretching) and static pressure. After vascular stent implantation, these three mechanical stimuli will change, and these changes are not immutable [6] [–] [8]. After implantation, the mechanical environments of blood vessels will undergo complex changes, and they vary with the process of vascular repair progressing. During stent implantation, with the expansion of stent wire, the changes in vascular mechanical environment are mainly those in static pressure and tension. With the prolonged stent implantation time, intimal thickening and the changes in lumen hemodynamics will become more prominent. Shear stress is the major cause of changes in the mechanical stimulation response of vascular endothelial cells. In the late stage of stent implantation, the static pressure on vascular endothelial cells will decrease with the degradation of bioresorbable scaffold struts.

The function of endothelial cells will be affected by these mechanical stimuli. Vascular inflammation, excessive proliferation and apoptosis of

* Corresponding author.
** Corresponding author.
E-mail addresses: wanggx@cqu.edu.cn (G. Wang), tieying_yin@cqu.edu.cn (T. Yin).

https://doi.org/10.1016/j.mtbio.2022.100410
Received 23 June 2022; Received in revised form 20 August 2022; Accepted 22 August 2022
Available online 27 August 2022

ECs can be induced by extremely low shear stress, which leads to the increase in arterial permeability to cholesterol-rich lipoproteins, thus inducing atherosclerosis (AS) [9]. Long-term increased hydrostatic pressure (i.e. hypertension) can lead to cardiovascular dysfunction, AS and organ damage [10]. At the cellular level, hydrostatic pressure has a physiological stimulating effect on ECs, which is a mechanical stimulation independent of shear stress and wall tension. Long-term elevated pressure will lead to an overall increase in the formation of F-actin and the deficiency of endothelial barrier function [11]. Sustained stretching can increase the permeability of vascular endothelial cells [12].

The connections between adjacent ECs involve TJs, adhesive junctions and gap junctions [13,14]. The fact that adhesive junctions make mechanical connections between adjacent cells, gap junctions provide intercellular communication, and TJ is a closed intercellular space is extremely important for the maintenance of the normal physiological function of blood vessels [15]. TJs play a decisive role in realizing vascular barrier function, with their restricting the free diffusion of molecules between cells (gate function) and serving as a membrane fence that limits the mixing of apical and basolateral plasma membrane domains (palisade function) [16,17]. TJPs between vascular ECs mainly consist of Claudin family, Occludin, Tricellulin, Junctional adhesion molecules (JAMs) and Zonula Occludens (ZOs). ZO proteins are necessary for the formation of TJ, as they act as a scaffold protein binding and regulating the expression of cytoplasmic (cytoskeleton) and transmembrane components [18]. There are three members of the ZO family, ZO-1, ZO-2, ZO-3 [19]. Among them, ZO-1 is the most important [20], which can participate in the proliferation and growth of cells [21]. The absence or damage of ZO-1 will cause TJ to lose mechanical sensitivity [22]. Moreover, embryonic knockout of ZO-1 causes embryonic death at 8.5 days [23]. In terms of such cells as cardiac myocytes, ZO-2 can help maintain the normal function of cells by playing the role that ZO-1 fail to play [24]. Cytoplasmic regions of a family of membrane proteins, Cluadin, are connected to ZOs and play a key role in regulating cell permeability [25]. Occludin participates in the regulation of cellular barrier function and plays an important role in maintaining the quality and function of TJ, but it is not a must for the formation of TJ [26]. Tricellulin is built at the top of the intersection of three cells and is an ideal place for controlling cell shape and coordinating multicellular movement. Tricellulin forms a barrier to macromolecules in tricellular TJs without affecting ion permeability [27]. A new study shows that it can be used to evaluate the maturity of TJPs in endothelial monolayers [28].

Mechanical stimulation affects the function of endothelial cells and even changes vascular permeability, and as a result, it is essential to focus on the effects of different kinds of mechanical stimulation on TJPs. Recently, some studies have shown that the expression of ZO-1 protein is affected by mechanical stimulation [22,29], while the expressions of other TJPs are rarely reported to be affected. Through investigating into the expressions of TJPs after PLLA bioresorbable scaffolds implantation, this study fills the gap of exploring the relationship between TJPs expression and mechanical stimulation.

2. Materials and methods

2.1. Experimental materials

After purchase from Army Medical University Animal Experiment center, SD rats (6 months old, 18 months old) were fed on a normal diet. 8-week-old male ApoE$^{-/-}$ mices were purchased from Army Medical University Animal Experiment center. After one week of adaptive feeding, the mice underwent partial carotid ligation [30] and were fed with western diet 8 weeks. The green fluorescent protein zebrafish (Flk1: GFP), in which endothelial cells express GFP, were provided by the Developmental Biology Laboratory at Tsinghua University. Zebrafish 1.5 days old were selected and placed in baby water containing 0.24 mg/ml Tricaine(Sigma, CAS:E10521) when they were raised to 2.5 days and 3.5 days, they were killed and their total RNA was extracted. All animals used in accordance with the guidelines of the Chinese Animal Care and Use Committee standards. Moreover, Laboratory Animal Welfare and Ethics Committee of Chongqing University approved all animal procedures for Animal Protection.

PLLA scaffolds (Φ2.0 × 13 mm, strut thickness 150 μm) were manufactured by Beijing Advanced Medical Technologies, Ltd Inc. (Beijing, China) using a proprietary 3-D printing technology [31]. Human umbilical vein endothelial cells (HUVECs) were all purchased from Cell Bank of Chinese Academy of Sciences.

2.2. In vivo scaffold implantation/balloon injury

In the implantation experiment, under aseptic conditions, after general anesthesia (10% chloral hydrate (Macklin, CAS: 302-17-0) and systemic anticoagulation, the abdominal aorta was surgically exposed. Then, a PLLA scaffold was deployed in the abdominal aorta of SD rat using a PTA balloon catheter, respectively. Balloons were inflated with 8 atm (nominal pressure) for 30 s to deploy the scaffolds. Aspirin (Bayer, 10 mg/kg/day) and Clopidogrel (Lepu Pharmaceuticals, Inc., 7.5 mg/kg/day) were started 3 days before angioplasty and continued 7 days. After 1week, 1 month, 3 months and 1year, post-implantation scaffolds were taken out and the arteries gently flushed with heparinized saline. One section was fixed in 4% paraformaldehyde (Servicebio, lot: G1101-500 ML) for histomorphometric staining. The other section of stented arteries was fixed with 2.5% glutaraldehyde (Hefei TNJ Chemical Industry Co., Ltd. China, CAS: 111-30-8) for scanning electron microscopic (SEM).

The experimental process of balloon injury is basically the same as that of scaffold implantation. The only difference is that when the balloon were inflated, it needs to be repeated 3 times to ensure damage.

2.3. Evans blue staining

Each time point after scaffolds implantation/balloon injury, with 1 mL of solution containing 2% Evans blue dye (Solarbio, CAS: 314-13-6) via tail vein injection by standard procedures as previously described [32]. The arteries containing the scaffold were harvested 1 h after the dyeing cycle, and the heart was perfused with 0.9% heparinized saline. Then the stented arteries were cut along the longitudinal direction. Image analysis was performed.

2.4. Cell culture and mechanical stimulations

HUVECs cultured with RPMI-1640, contained 10% Fetal Bovine Serum (FBS, Wisent Bioproduction, Cat: 086–150) in a 5% CO_2, 37 °C incubator, respectively. For mechanical stimulations, HUVECs were loaded with 20, 30, 40 KPa static pressure through airtight high pressure device (Chongqing University) for 6 and 12 h. HUVECs were exposed to 6, 12, 25 and 35 dyne/cm^2 shear stress for 6 h by a parallel plate flow chamber (Beijing Aerospace University). HUVECs were loaded with a periodic tension (5% and 10%, 1 Hz) for 12 h by Flexcell 4000 T (Flexcell International, USA).

2.5. Immunofluorescence

Anti-ZO-1 antibody (ZO1-1A12, ThermoFisher, 1:200 dilution), anti-CD31 (GB13248, ServiceBio, 1:3000 dilution), anti-Occludin (OC–3F10, ThermoFisher, 1:500 dilution), anti-Claudin-5 (Ab-AF0130, Affinity, 1:300 dilution), anti-Tricellulin (48–8400, ThermoFisher, 1:100 dilution), anti-VE-cadherin (36–1900, ThermoFisher, 1:50 dilution) and phalloidin labeled F-actin (A30106, ThermoFisher, 1:400 dilution) were used for immune-fluorescent staining, the second antibodies used were goat anti-mouse IgG H&L (ab150113, Abcam, Alexa Fluor® 488, 1:200 dilution) and donkey anti-rabbit IgG H&L (ab150075, Abcam, Alexa Fluor® 647, 1:200 dilution). Paraffin sections were sealed with 1% bovine serum albumin (Solarbio, CAS:A8010) for 1 h. The first antibody was incubated at 4 °C for 12 h. The second antibody, DAPI (Solarbio,

CAS: 28718-90-3) and phalloidin labeled F-actin were incubated at room temperature for 1 h. After each incubation, wash with PBS (Servicebio, lot: G0002-2L) for 3 times, each time for 10 min. For immuno-fluorescent observation, Leica SP8 confocal microscope was applied. The captured data are imaged by LAS_X_2.0.2_15022, and then ImageJ is applied for fluorescence statistics.

2.6. SEM

The samples were fixed with 2.5% glutaraldehyde and left for 12 h. Subsequently these were dehydrated using a series of gradient solutions of 30%, 50%, 70%, 80%, 90%, 100%, and 100% *tert*-butyl alcohol (Jinan Finer Chemical Co., CAS: 75-65-0) with each step lasting 15 min. Before shooting, place it on the conductive tape (Nisshin EM, Japan). Maintain a vacuum of 0 °C during scanning. SEM was performed with a Hitachi SU3800, this was operated at 10–15 kV to examine the endothelialization of the implanted artery lumen surfaces.

2.7. RNA extraction and quantitative PCR analysis

Total RNA was extracted using TRIzol reagent (Takara). Reverse transcription was performed using a PrimeScript™ RT reagent Kit (Takara) with gDNA Eraser. TB Green Premix Ex Tap^{TM} II (Tli RNaseH Plus) (Takara) was used for quantitative real-time PCR with the Bio-Rad CFX 96 (Bio-Rad, Hercules, CA, USA). Quantitative PCR analysis was performed with Human GAPDH as the internal control. Relative changes in gene expression levels were quantitated based on three biological replicates via the $2^{-\Delta\Delta Ct}$ method.

2.8. Statistical analysis

Statistical analyses were performed with Statistical Package for GraphPad Prism 6 software. Differences in multiple groups with one variable were determined by using one-way ANOVA (analysis of variance) followed by two-tailed Student's *t*-test. All the sample sizes were proved to be appropriate for assumption of normal distribution and variance was similar between the compared groups. The values of mean determinants are presented as mean ± SD. Significant differences between groups were set at * $p < 0.05$ **, $p < 0.01$***, $p < 0.001$.

3. Results

3.1. The abdominal aortic permeability recovered at 3 months after PLLA bioresorbable scaffold implantation

After PLLA scaffolds were implanted into the abdominal aorta of 6-month-old male SD rats, 1 week, 1 month and 3 months were selected as time points for sampling observation (Fig. 1A). It was found that after PLLA scaffold implantation and Evans blue staining of the samples, the permeability of abdominal aorta increased first and then decreased, which shows a state of gradual repair (Fig. 1B). The dye was observed to be almost distributed in the whole BRSs segment one week after BRSs implantation. The colors of both ends of the BRSs were darker than that of the middle area, and the surrounding areas of the BRSs struts were basically dyed blue. 1 month after implantation, the dye diffused throughout the scaffold, but the staining was lighter than that of one week after implantation. Three months after implantation, the dye was only stained on both ends of the scaffold, and the color of the rest parts was close to that of the control group. The results showed that the vascular permeability was destroyed after PLLA scaffolds implantation, and the barrier function gradually recovered after one week and returned to near normal after three months (Fig. 1C). The recovery of vascular permeability is related to the self-repair of endothelial monolayers, which was verified through SEM observation (Fig. 1D). A positive correlation was found between ECs growth time and intimal coverage. One week after implantation, the scaffold strut was basically exposed. One month after implantation, some parts of the scaffolds were covered by a thin layer of neointima. Three months after implantation, most part of the middle area of the scaffold was completely covered by neointima, but the outline of the scaffold strut could be seen at both ends of the blood vessel. At this time, the cells on the scaffold surface presented a clear outline, and orderly arrangement could be observed. This indicates the barrier function of endothelium has been basically recovered.

These results suggest that PLLA scaffolds implantation has caused vascular endothelia damage, especially at both ends of the scaffolds and at the position of the scaffold struts. The damage was significant and the osmosis increased significantly. The recovery of permeability of abdominal aorta will be gradually achieved through ECs regeneration.

3.2. The differential expression levels of TJPs after PLLA scaffolds implantation

In order to verify the relationship between vascular permeability and expression of TJPs, immunofluorescence staining of paraffin sections were carried out each time. We performed statistics and analysis on TJPs that were located in the neointima (the area between the edge of the vascular lumen and the first elastic plate). The results show that the expression level of ZO-1 decreased at 1 week after implantation, and then increased gradually. At the third month, the expression level reached its peak, and it became lower after one year. (Figs. 2A, B, S1). After BRSs implantation, there was no significant difference in the expression level of Claudin-5. However, there was a significant decrease in the expression level at 3 months and 1 year compared with that at 1 week and 1 month. (Fig. 2A, C). The expression level of Occludin, close to the level of control group, was the highest at 1 month, and significantly lower at 3 months and 1 year (Fig. 2A, D). After BRSs implantation, the expression level of Tricellulin was lower than that in the control group (Fig. 2A, E). It is worth noting that the expression level of TJPs in neointima ECs is different from those of TJPs in the whole neointima. The expression levels of TJPs in neointima ECs reflect the recovery of endothelial function at the cellular level, while the expression level of TJPs in neointima can reflect the endothelial function at the tissue level. From these results, the overall expression levels of the four TJPs are closely related to vascular permeability. TJPs, affected by implantation injuries and continuous intense stimulation, participates in ECs repair, thereby affecting vascular permeability.

The expressions of these TJPs show different trends at each time point after PLLA BRSs implantation, and each expression does not follow the same trend. In terms of BRSs implantation, the mechanical stimulation factors for changes in vascular physiological environment mainly involve tension, shear stress and static pressure enhancement. After that, with the thickening of neointima, the shear stress will change mainly. With the degradation of scaffolds, the mechanical related factors in the local range of blood vessels changed. Cells respond to these factors, thus leading to subsequent changes. Therefore, this is speculated to be related to the diversity, continuous change and comprehensive effect of vascular mechanical environment. From the expression levels of TJPs after BRSs implantation, except that the expression change of ZO-1 is consistent with the recovery of vascular permeability, the expression trends of the other three TJPs cannot be explained with a single factor. As a result, the expression changes of TJPs were analyzed in other models.

3.3. The expression levels of TJPs in other in vivo models were different from those of TJPs in BRSs implantation

In the process of BRSs implantation and degradation, vascular mechanical environment changes with time passing by. In order to verify that the expression levels of TJPs are related to continuous mechanical

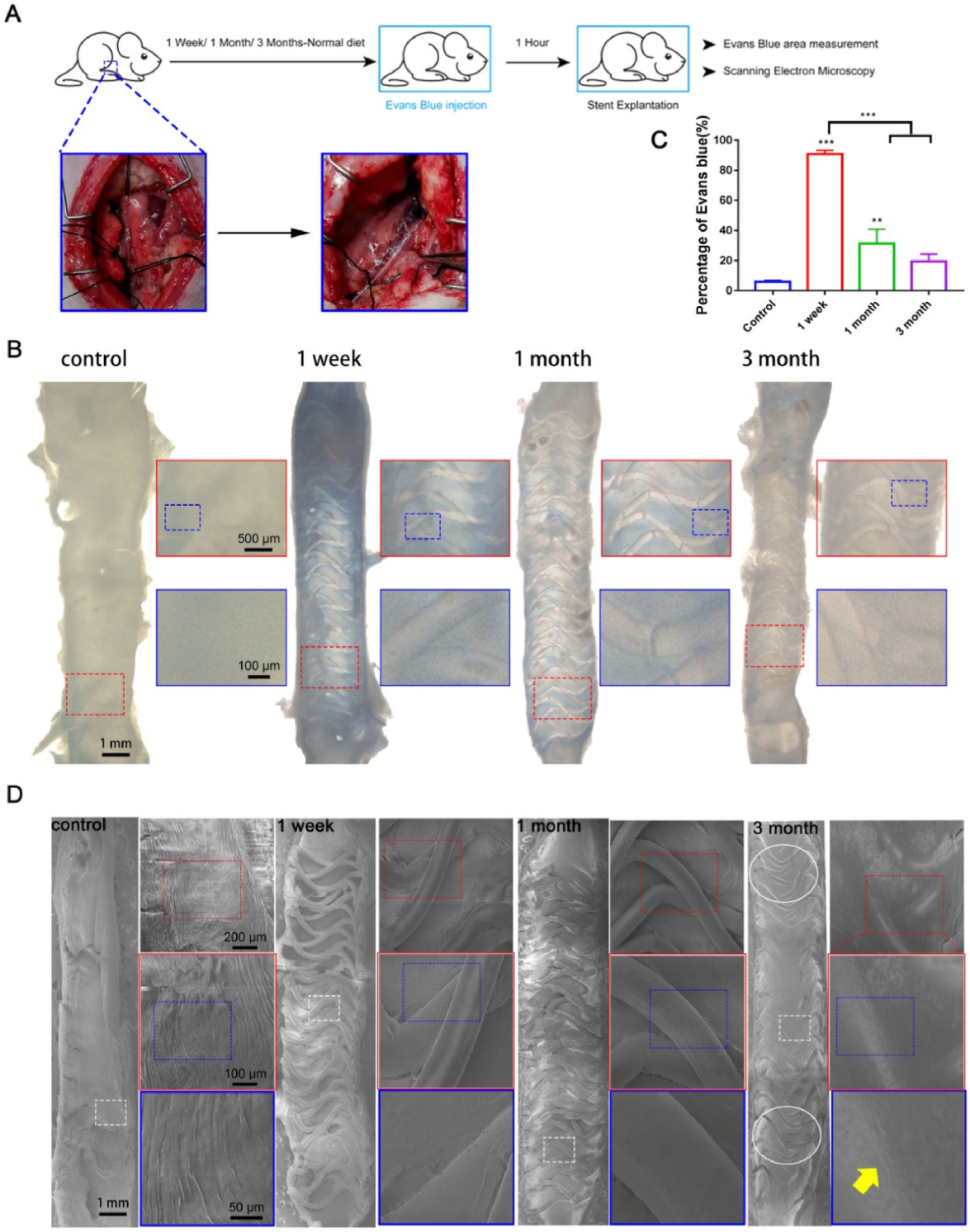

Fig. 1. The abdominal aortic permeability after PLLA scaffolds implantation in rats. (A) During the animal experiment, PLLA scaffolds were implanted into the abdominal aorta of male SD rats. Samples were taken at 1 week, 1 month and 3 months respectively; (B) results of Evans blue staining rat abdominal aorta; (C) the proportion of Evans blue staining area to the total vascular area; (D) SEM observation of rat abdominal aorta. White ellipse indicates the outline of the BRSs struts in both ends of the PLLA scaffold at 3 months, with orderly arranged cells on the scaffold surface (yellow arrow). $^{**}p < 0.01$, $^{***}p < 0.001$. (For interpretation of the references to color in this figure legend, the reader is referred to the Web version of this article.)

changes, we observed the expression of TJPs in rat abdominal aorta after balloon injuries. The expression levels of 3 TJPs were found to have decreased first and then to have increased after balloon injuries (Fig. 3A–D). The expression level of Tricellulin was the highest within the first month, and no significant change was observed afterwards (Fig. 3E). This indicates that the expression of TJPs gradually recovered with time passing by after transient endothelial injuries. Unlike the results of BRSs implantation, the expression trends of TJPs in the neointima ECs here are the same as that of the whole. From the above results, we can see that the four TJPs reflect a simple repair expression after balloon injuries.

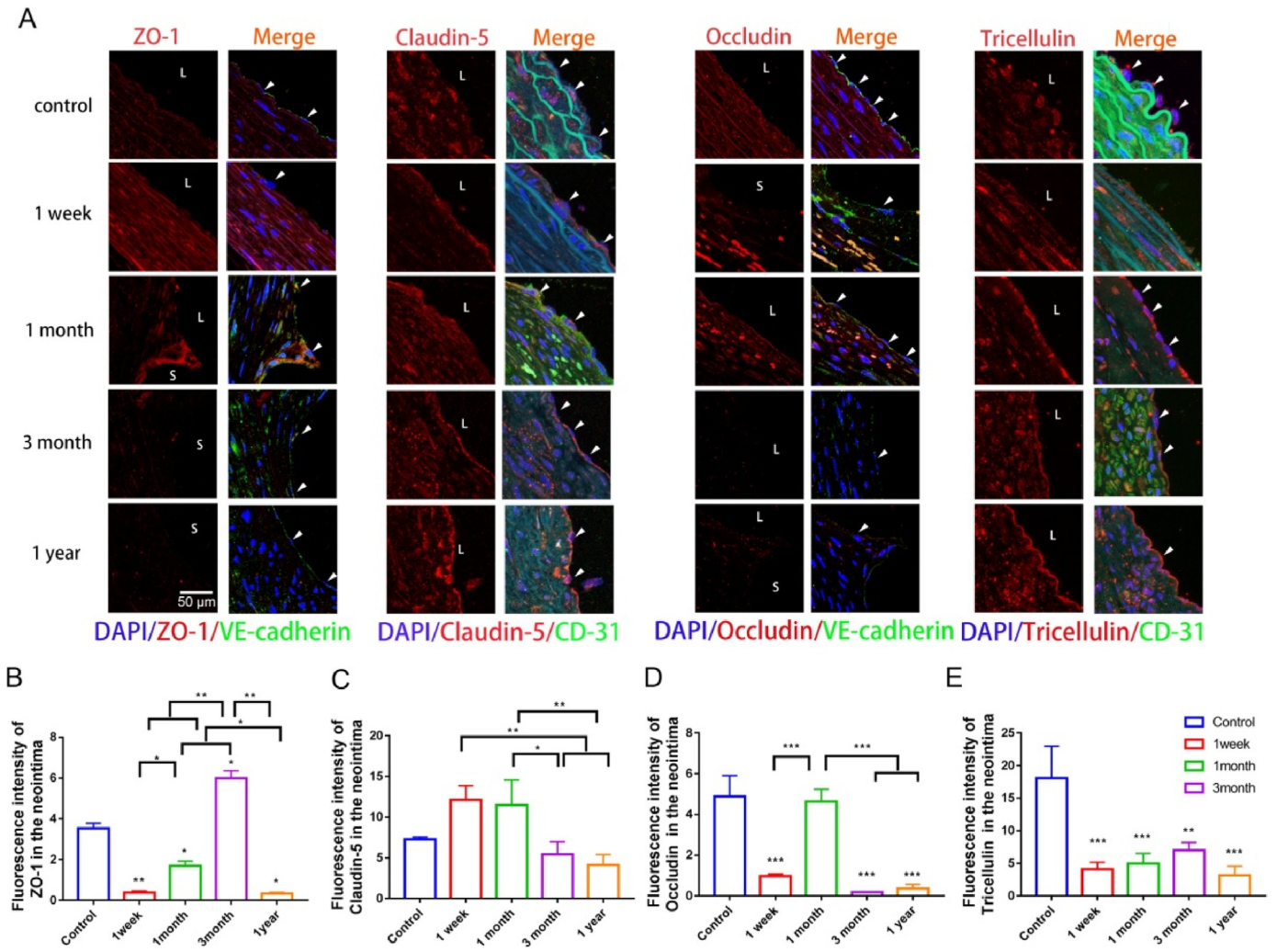

Fig. 2. The differential expression of TJPs in the neointima of abdominal aorta after implantation of PLLA scaffold in rats. (A) Immunofluorescence staining of paraffin sections of abdominal aorta of rats implanted with PLLA scaffold (white arrows: ECs with higher expression level of TJPs, S: the scaffold strut, L: the lumen); (B-E) statistics of immunofluorescence staining intensity of ZO-1(B), Claudin-5(C), Occludin(D) and Tricellulin(E) in the neointima of sections. < 0.05, $^{**}p < 0.01$, $^{***}p < 0.001$.

Evans blue staining was performed on blood vessel samples collected after balloon injuries. It was found that the overall condition was similar to that after BRSs implantation, but the degree of injury was slightly lower (Fig. 3F and G). This proves that BRSs implantation is not the decisive factor affecting vascular permeability, and endothelial injury and repair are the key factors affecting vascular permeability. The injury after PLLA scaffolds implantation was more serious than the balloon injury at one week, but the recoveries were similar to each other at one month. This shows that mechanical factors accelerate the repair of endothelial injuries. This once again verifies the fact that the repair process after vascular injury is realized by mechanical factors through affecting the expression level of TJPs.

In addition, we also observed the effect of mechanical stimulation on the expression of TJPs in other animal models. Except Claudin-5, other TJPs showed significant expression changes in zebrafish blood vessels after Tricane treatment (Fig. 3H). Tricane can decrease the heart rate of zebrafish, thus inducing the lower shear stress in its blood vessels. In the atherosclerotic lesion model of partial carotid artery ligation in ApoE$^{-/-}$ mice, three kinds of TJPs except ZO-1 significantly increased in the left carotid artery with mechanical stimuli changing (Fig. 3I). These results further suggest that mechanical stimulation can regulate the expression of TJPs. However, the changes in mechanical factors in vivo are relatively complex. In order to thoroughly analyze the relationship between various mechanical factors and various TJPs, we carried out mechanical loading experiments in vitro.

3.4. *In vitro differential mechanical stimulation can induce differential expression of TJPs*

In order to further illustrate that the changes in TJPs expression level after BRSs implantation are caused by mechanical factors, human umbilical vein endothelial cells (HUVECs) were mechanically loaded in vitro to observe the changes in expression levels of TJPs after mechanical stimulation. First of all, tensile forces of 5% and 10% were applied to load the cells for 12 h. Tricellulin was significantly up-regulated under both tensile conditions. However, different from the other mechanical stimulation, the stretching force mainly caused significant down-regulations of the expression levels of other TJPs (Fig. 4A). It is worth noting that although their expression trends were down-regulated, the down-regulation degrees of ZO-1, Occludin and Claudin-5 were different with the differences in tensile strength. Next, we chose the static pressures of 20, 30 and 40 KPa to load the cells for 6 h. This time, the situation is not the same as that after shear stress loading (Fig. 4B). The expression levels of all TJPs increased significantly after loading at 40 KPa. The expression

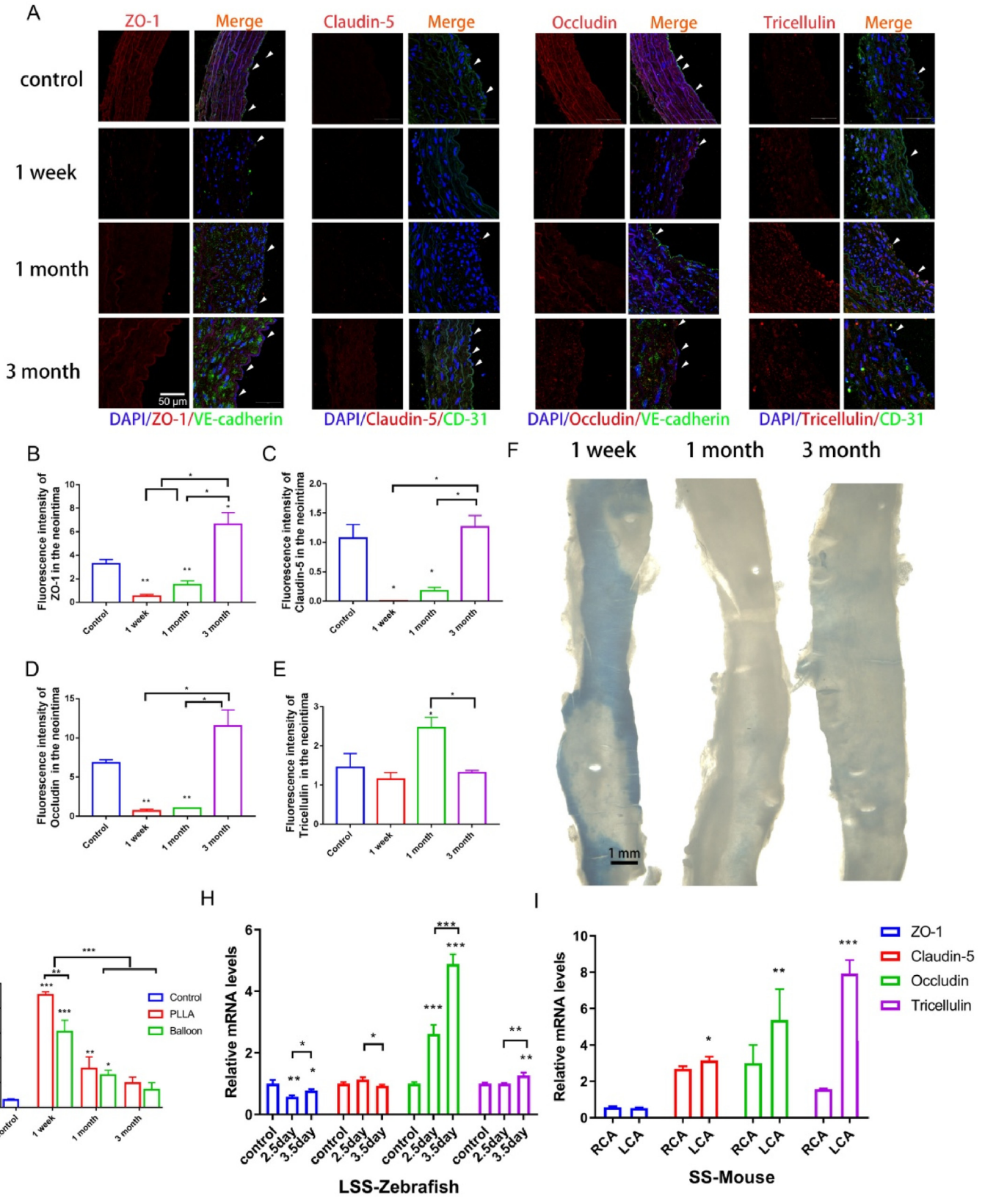

Fig. 3. Mechanical stimulation is an important factor for the changes in the expression levels of TJPs after different intravascular injuries. (A) Immunofluorescence staining of paraffin sections of rat abdominal aortic balloon injury (white arrow: neointima ECs); (B-E) statistics of immunofluorescence staining intensity of ZO-1, Claudin-5, Occludin and Tricellulin in sections;(F) Evans blue staining results of rat abdominal aorta; (G) the proportion of Evans blue staining area to the total vascular area; (H,I) real-time fluorescence quantitative PCR results of ZO-1, Claudin-5, Occludin and Tricellulin after zebrafish drug treatment (H) and partial carotid artery ligation in ApoE$^{-/-}$ mice (I). *$p < 0.05$, **$p < 0.01$, ***$p < 0.001$. (For interpretation of the references to color in this figure legend, the reader is referred to the Web version of this article.)

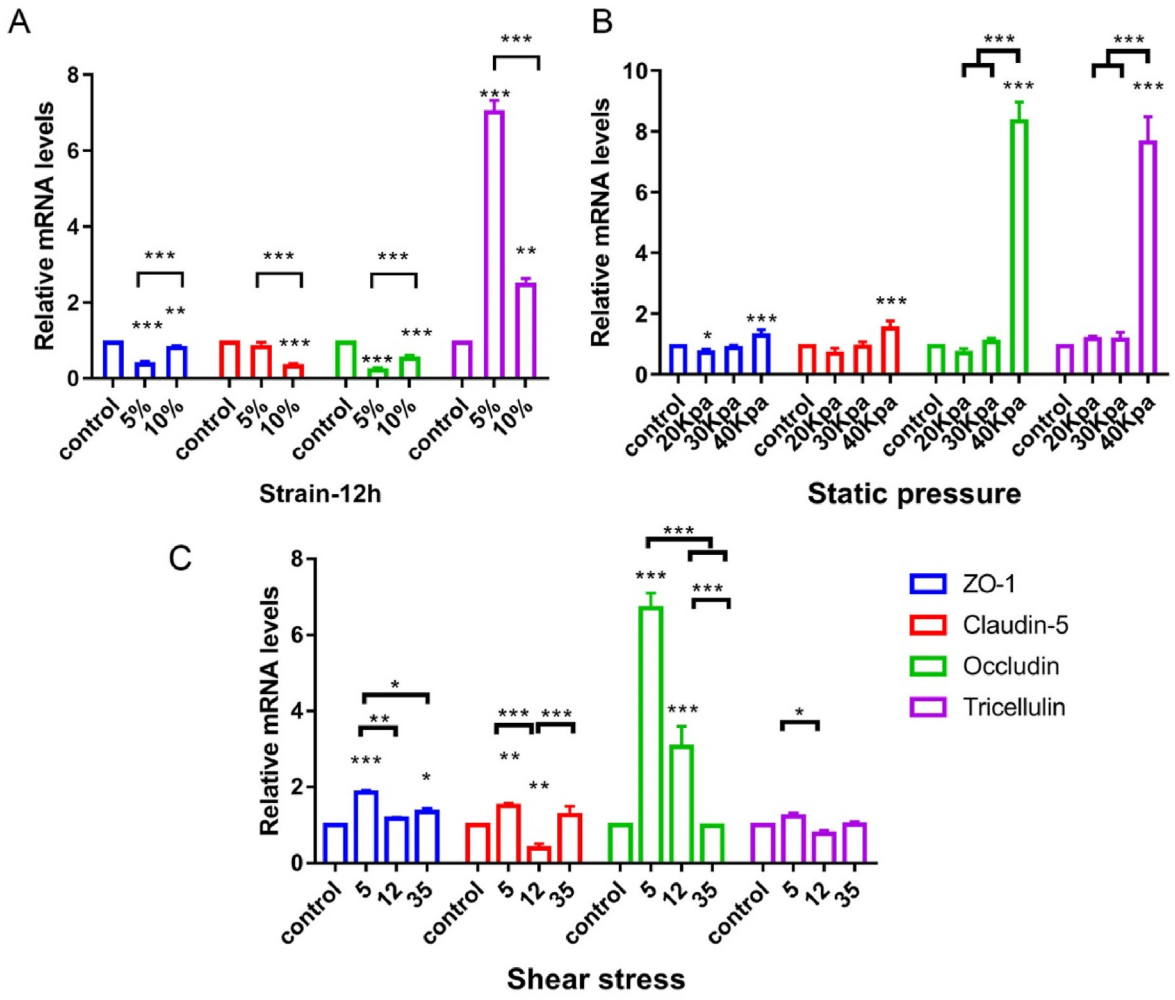

Fig. 4. Differential mechanical stimulation induce differential expression levels of TJPs. (A-C) Real time fluorescence quantitative PCR results of ZO-1, Claudin-5, Occludin and Tricellulin of human umbilical vein endothelial cells after different tensile, static pressure and shear loadings. *p < 0.05, **p < 0.01, ***p < 0.001.

of ZO-1 decreased significantly at 20 KPa, but no significant change was observed at 30 KPa. The expression levels of the other three TJPs did not change significantly under these two conditions.

Finally, we selected shear stresses of 5, 12, and 35 dyn respectively to load the cells for 6 h. We observed that the expression levels of various TJPs showed different changes under different shear forces (Fig. 4C). ZO-1 responds to the shear stresses of 5 and 35 dyn, which shows a significant increasing trend under these conditions. The expression of Claudin-5 was affected by various shear forces. Under the two extreme shear stress environments of 5 and 35 dyn, the expression level increased significantly. However, the expression level was significantly decreased at 12 dyn. Occludin only responded to the shear stresses of 5 dyn and 12 dyn, and its expression level increased significantly under these conditions.

These results show that the expression levels of TJPs are affected by mechanical stimulation, but the effects of different kinds and strengths of mechanical stimulation on the expression levels are different. ZO-1 is more sensitive to shear stress and tension than to static pressure. Compared with the control, the mRNA expression level of ZO-1 at 5 dyn was increased nearly twofold. Moreover, the mRNA expression level of ZO-1 was reduced to about 43% under 5% stretching. ZO-1 is sensitive to tension, but is negatively regulated under stretching. Occludin is sensitive to static pressure and shear stress. Compared with the control, the mRNA expression level of Occludin increased more than 6-fold at 5 dyn and more than 8-fold at 40 KPa. Tricellulin is more sensitive to stretching. Compared with the control, the mRNA expression level of Tricellulin was increased more than 2-fold under 5% stretching and more than 7-fold under 10% stretching. Although the expression level of Tricellulin was significantly increased at 40 KPa, it was not corresponding at 20 and 30 KPa. Therefore, we believe that Tricellulin is more sensitive to tension than static pressure. Compared with the other three TJPs, Claudin-5 can respond to mechanical stimulation, but the sensitivity is relatively low. Therefore, the fact that the sensitivities of the four TJPs to different types of mechanical stimuli are different may be the main reason for their differential expression levels.

From the results of endothelial injury models in vivo and loading experiments in vitro, the following conclusions can be drawn. In the two models, the overall expression trends of ZO-1 were similar to each other; the significant decrease of Occludin expression three months after BRSs implantation may be caused by the changes in shear stress. The expression trend of Claudin-5 was the most special, and it may also be affected by other factors. The expression levels of Tricellulin in the balloon model were close to or higher than those of the control at each stage, while the expression level was lower than that of the control after BRSs implantation. The support of the BRSs provides a relatively stable tensile environment for the blood vessels, which indicates that Tricellulin responds to periodic tension rather than to constant tension.

3.5. *In vitro mechanical stimulation affected cell morphology*

Vascular permeability is not only affected by the expression levels of TJPs, but also related to the morphological changes of endothelial cells. In order to investigate into the effect of mechanical factors on cell

morphology, we observed the morphology of endothelial cells after mechanical loading through the use of SEM and immunofluorescence staining. SEM observation results showed that the morphology of HUVECs in the control group was fusiform, with smooth surface and outward convex trend, clear cell edge texture and close contact between adjacent cells, and that the morphology of HUVECs in the treatment group was flat, with uneven cell surface, pseudopodia at the edge of cells and pores between adjacent cells (Fig. S2A). After the 12-h loading at 40kpa, we found that the morphology of HUVECs became narrow and long, the surface of cells was uneven, there were many pseudopodia at the edge of cells, there were gaps between cells, and there was dispersed distribution of cells (Fig. S2B).

Through immunofluorescence staining, the cytoskeleton of endothelial cells was also found to have changed significantly after mechanical loading. We could clearly observe that mechanical loading did not affect the expression of CD31. However, the expression of F-actins was down regulated. In the control group, F-actin presented a regular shape similar to a "triangle", with clear edges and corners. They were evenly distributed in the cells, and the close arrangement between cells and without obvious pores. After the 6-h loading at 40kpa, a small amount of pseudopodia (white arrow) appeared in the cells. However, there was no significant difference in the expression of F-actins (Figs. S3A and D). If the loading time was extended to 12 h, the expression of F-actins increased (Figs. S3B and E). We observed that the fluorescence intensity of F-actins at the edge of the cells was higher than that in the middle of the cells, and there was a tendency of transferring to the cell membranes. There were many pseudopodia at the edges of the cells, and there were obvious pores between cells. After the 6-h 5 dyne loading, the fluorescence intensity of F-actins decreased significantly (Figs. S3C and F). These results show that mechanical stimulation can affect cell morphology by affecting the expression of F-actins, but it does not affect the activity of endothelial cells in this process. At the same time, mechanical stimulation can change the morphology of endothelial cells and increase the gap between cells, thus affecting the function of endothelial barrier.

3.6. The levels of inflammation may also be one of the factors affecting the expression levels of TJPs

With the function of vascular barrier destructed, the invasion of inflammatory cells increased. Therefore, attention should be paid to the inflammation of blood vessels at this time. Through immunohistochemical staining, we found that after BRSs implantation, the inflammation level of abdominal aorta increased at first and then decreased, and reached the peak at one month after BRSs implantation (Fig. 5A). From the analysis of the expression levels of four compact proteins, we found that only the expression of Claudin-5 was different from those of the other three proteins, and it was related to the level of inflammation. In a normal vascular physiological environment, the vascular wall consists of intima, media and adventitia which is thicker and contains more SMCs, and adventitia which is composed of loosely connected tissues. The vascular wall includes intima, media and adventitia, which is thicker and contains more SMCs; adventitia, which is composed of loose connective tissue. Intimal hyperplasia after BRSs implantation is an important index of endothelial function evaluation. Therefore, we carried out HE staining on the samples collected at each time point. Through HE staining (Fig. 5B), we observed that a small amount of neointima appeared and a small number of blood cells adhered to the blood vessels 1 week after BRSs implantation. After that, the neointima gradually thickened, then peaked at three months after implantation, with the company of partial inflammatory cell infiltration (black arrow). One year after implantation, the vascular diameter of the BRSs segment significantly reduced, and the neointima thickness and inflammatory cell infiltration were less than the results observed at three months after implantation. After a balloon injury, neointima was more obvious only within one month after the balloon injury, with less inflammatory cells infiltrated. Subsequently, we counted the number of neointima areas observed at each time point after implantation, and we observed that the neointima areas of the blood vessels increased gradually after PLLA scaffold implantation (Fig. 5E). Three months after the balloon injury, neointima basically recovered to the level before the injury (Fig. 5F). In order to evaluate intimal hyperplasia in more detail, we stained the samples with immunofluorescence and selected high multiple for observation (Fig. 5D, G, H). The results showed that after BRSs implantation, the neointima thickness increased gradually and reached the peak at 3 months. This is consistent with the previous HE staining results. However, it is worth noting that 1 year after implantation, the relationship between neointima thicknesses and areas is not proportional, which is speculated to be related to age-induced vasoconstriction. We observed the expression of TJPs in the blood vessels of aged rats (the age is equivalent to one year after BRSs implantation) (Fig. S4). The expression of ZO-1 was low in elderly blood vessels, and increased in the experimental group. The expression level of Claudin-5 was high in elderly blood vessels, which is presumed to be related to the level of inflammation.

4. Discussion

In different organizations, the main components of TJPs are slightly different. Here, we mainly focus on vascular ECs. Therefore, we chose four kinds of TJPs, ZO-1, Occludin, Cluadin5 and Tricellulin as our main research objects.

From the experimental results, the expression levels of TJPs can be found to be greatly affected by mechanical stimulation with the implantation of PLLA scaffold. However, the expression levels of the four TJPs have shown different trends under the conditions of different kinds and strengths of mechanical stimulation, which is related to own characteristics of the TJPs. From the balloon injury samples, we can see that the four TJPs take part in the repair of endothelial barrier function. But the expression trend of Tricellulin is different from those of the other three, which may be due to its role as an indicator of endothelial function repair. Therefore, one month after injury, during the critical period of initial recovery of endothelial barrier function, Tricellulin took the lead in increasing the expression level.

After BRSs implantation, the expression trend of Claudin-5 was also different from that of the other three TJPs. From the results of ICAM and VCAM immunohistochemical staining, Claudin-5 was found to present better inflammatory adaptability than the other three TJPs, which has been confirmed by other related studies. This shows that Claudin-5 is affected by mechanical stimulation and inflammatory factors, while the other three TJPs tend to be influenced by mechanical stimulation.

Occludin is the most sensitive to mechanical stimulation among the four TJPs. Under the same mechanical stimulation, Occludin expression showed the most significant sensitivity in the group. One month after BRSs implantation, intimal hyperplasia was the most serious, and the changes in low shear stress were the most prominent. The expression of Occludin showed a significant increase.

More noteworthy, however, is ZO-1. It seems to be the least special, but in fact it is precisely what makes it the most special. The expression of ZO-1 showed a trend similar to those of the other three TJPs under certain mechanical stimulations. What's more, a large number of literature [15,20] [–] [23,33] [–] [36] have shown that ZO-1 is the most important TJP, as its expression level can directly affect the other three. Although all four TJPs are subject to mechanical stimuli, they show different sensitivities to various mechanical stimuli. ZO-1 is more sensitive to shear stress and tension than to static pressure. Occludin is sensitive to static pressure and shear stress. Tricellulin is more sensitive to stretching.

After BRSs implantation, the static pressure and tension in the vascular lumen increased, and the shear stress changed correspondingly and continuously with intimal hyperplasia thickening. The expression levels of TJPs were significantly different after receiving transient injury and continuous mechanical stimulation. This suggests that the changes in mechanical stimulation are the key fctors for the differential expression

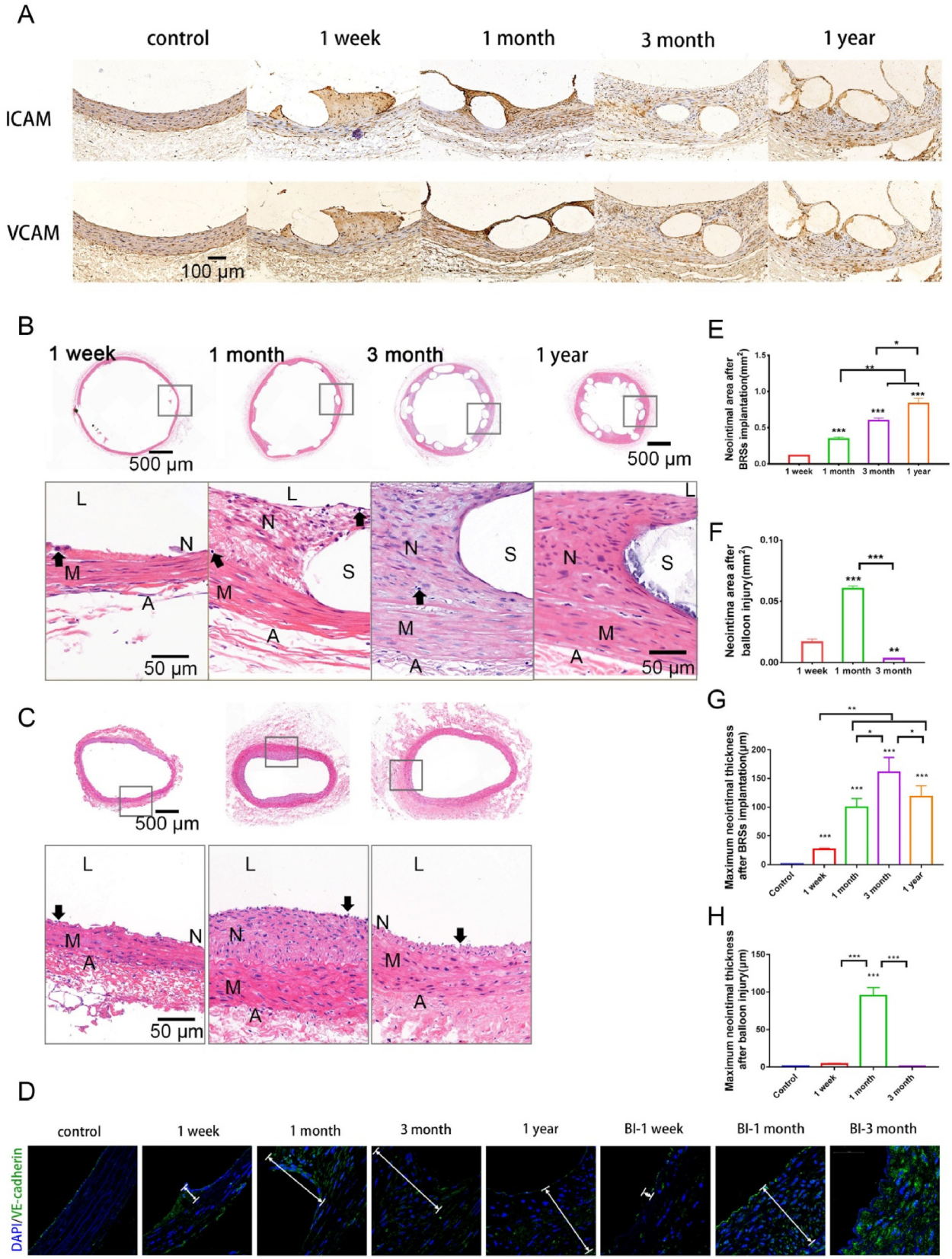

Fig. 5. The level of inflammation may also be one of the factors affecting the expression levels of TJPs. (A) Implantation of PLLA scaffold into rat abdominal aorta paraffin section ICAM, VCAM immunohistochemical staining; (B–C) implantation of PLLA scaffold into rat abdominal aorta paraffin section, rat abdominal aorta balloon injury paraffin section HE staining (black arrow: inflammatory cells, S: scaffold strut, M: media, N: neointima, A: adventitia and L represents the lumen); (D) implantation of PLLA scaffold into rat abdominal aorta paraffin section, rat abdominal active vein balloon injury paraffin section immunofluorescence staining (white arrow: thicknesses of neointima, BI: balloon injury) (E,G) according to Fig. 5B, statistics of neointima areas and thicknesses of abdominal aorta implanted with PLLA scaffold (F, H) according to Fig. 5C, statistics of neointima areas and thicknesses of abdominal aortic balloon injuries in rats. *$p < 0.05$, **$p < 0.01$,***$p < 0.001$.

levels of the 4 TJPs. In addition, mechanical stimulation can not only affect the expression of TJPs, but also accelerate the repair process of endothelium.

By comparing the samples collected at three months after BRSs implantation and those obtained at three months after a balloon injury, it is not difficult to find that the recovery degrees of vascular barrier function are similar to each other, but the expression trends of TJPs are different. This shows that the differential expression levels of TJPs are the factors greatly affecting the vascular barrier function, but they are not the only factors. Intimal thicknesses and inflammatory factors also continue to affect vascular barrier function. It is noteworthy that stent implantation is not directly related to the changes in the vascular permeability. It is the injury and repair of endothelium that cause the changes in vascular permeability.

According to existing studies, the degradation time of PLLA scaffolds in vivo is 2–4 years [37,38]. Igaki•Tamai stent is the first non drug coated self expanding biodegradable polymer stent made of PLLA for human clinical evaluation [39]. The clinical results showed that the stent was continuously expanded within 3 months after implantation, and the cross-sectional area of the lumen was reduced. After 3 months, the stent remained stable, and finally degraded completely within 36 months after implantation [40].

Stent implantation objects commonly used for research include human, rat, rabbit, monkey, dog and so on. After PLLA scaffolds were implanted into the abdominal aorta of rats, vascular repair involved two processes, "0–6 months" (characterized by inflammation, neointimal hyperplasia, and endothelial re-functionalization) and "after 6 months" (characterized by scaffold degradation and positive vascular remodeling) [32]. After PLLA scaffolds were implanted into the coronary artery of pigs, some scaffold struts were still visible after 3 years, and the complete scaffold struts could not be observed by optical coherence tomography until 4 years later [41].

This study shows that the expression levels of TJPs are affected by mechanical factors after BRSs implantation. There are still some shortcomings about this study: in-depth discussions on mechanism are not conducted; there is no more in-depth judgment on the intensities and types of mechanical stimulation at certain time points after implantation; no study has been conducted on the effect of other factors affecting the expression levels of TJPs after BRSs implantation. JAM are a class of cell–cell adhesion molecules that localize to TJs. JAM-A, JAM-B, and JAM-C are known, and play important roles in regulating the epithelial barrier and polarity [34]. Moreover, research shows that ZOs can recruit Occludin and Cluadins, but not JAM-A [42]. Therefore, although JAMs have important functions for TJ, we do not take them as the main research object. Anyway, this is a prelimnary study attempting to start the investigation into the relationship between the expression levels of connexins and mechanical stimulations. It is believed that in the future, through further explorations, more will be found about the relationship between mechanical stimulations and vascular endothelial barrier function.

5. Conclusions

Vascular permeability is found to be determined by the expression levels of TJPs and neointima thicknesses after BRSs implantation. In this process, the mechanical stimulations play an important role in regulating vascular barrier function. Different TJPs show different sensitivities to different types of mechanical stimuli, which is the key factor for the heterogeneous expression levels of TJPs. This not only helps start a new research direction for the analysis of complex vascular physiological environmental factors, but also provides a new reference for improving the design of BRSs. Furthermore, this study shows that TJPs can be used as a new target of drug loaded coating for dealing with the impairment of vascular barrier function after BRSs implantation.

Credit author statement

Junyang Huang: Investigation, Formal analysis, Writing – original draft. Shuang Ge: Investigation, Formal analysis. Desha Luo: Investigation, Formal analysis. Ruolin Du: Investigation. Yang Wang: Investigation. Wanling Liu: Investigation. Guixue Wang: Resources, Funding acquisition, Supervision, Project administration, Writing – review & editing. Tieying Yin: Conceptualization, Methodology, Resources, Supervision, Project administration, Funding acquisition, Writing – review & editing.

Funding

This study was supported by the Key and general projects of National Natural Science Foundation of China (12032007), the Key and general projects of Natural Science Foundation of Chongqing (cstc2019jcyj-zdxmX0009, cstc2019jcyj-zdxmX0028, cstc2019jcyj-msxmX0307).

Data availability statement

The raw/processed data required to reproduce these findings cannot be shared at this time as the data also forms part of an ongoing study.

Declaration of competing interest

The authors declare that they have no known competing financial interests or personal relationships that could have appeared to influence the work reported in this paper.

Acknowledgements

We gratefully thanked the other staff of the Public Experiment Center of State Bioindustrial Base (Chongqing) for providing technical support and assistance in data collection and analysis. The authors would like to thank Dr. Qing Liu at Beijing Advanced Medical Technologies Inc. for his kind assistance of 3-D Printed PLLA Scaffolds.

Appendix A. Supplementary data

Supplementary data to this article can be found online at https://doi.org/10.1016/j.mtbio.2022.100410.

References

[1] R. Du, Y. Wang, Y. Huang, Y. Zhao, D. Zhang, D. Du, Y. Zhang, Z. Li, S. McGinty, G. Pontrelli, T. Yin, G. Wang, Design and testing of hydrophobic core/hydrophilic shell nano/micro particles for drug-eluting stent coating, NPG Asia Mater. 10 (2018) 642–658, https://doi.org/10.1038/s41427-018-0064-z.

[2] W. Khan, S. Farah, A.J. Domb, Drug eluting stents: developments and current status, J. Contr. Release 161 (2012) 703–712, https://doi.org/10.1016/j.jconrel.2012.02.010.

[3] T. Hu, J. Yang, K. Cui, Q. Rao, T. Yin, L. Tan, Y. Zhang, Z. Li, G. Wang, Controlled slow-release drug-eluting stents for the prevention of coronary restenosis: recent progress and future prospects, ACS Appl. Mater. Interfaces 7 (2015), https://doi.org/10.1021/acsami.5b01993.

[4] Y. Wang, H. Wu, W. Zhen, T. Gong, D. Li, Y. Cai, S. Fan, [Research progress of biodegradable vascular stent], Zhongguo Yi Liao Qi Xie Za Zhi 45 (2021) 410–415, https://doi.org/10.3969/j.issn.1671-7104.2021.04.013.

[5] R.A. Byrne, M. Joner, A. Kastrati, Stent thrombosis and restenosis: what have we learned and where are we going? The Andreas Grüntzig Lecture ESC 2014, Eur. Heart J. 36 (2015) 3320–3331, https://doi.org/10.1093/eurheartj/ehv511.

[6] P.S. Zun, A.J. Narracott, C. Chiastra, J. Gunn, A.G. Hoekstra, Location-specific comparison between a 3D in-stent restenosis model and micro-CT and histology data from porcine in vivo experiments, Cardiovasc Eng. Technol. 10 (2019) 568–582, https://doi.org/10.1007/s13239-019-00431-4.

[7] K.C. Koskinas, Y.S. Chatzizisis, A.P. Antoniadis, G.D. Giannoglou, Role of endothelial shear stress in stent restenosis and thrombosis: pathophysiologic mechanisms and implications for clinical translation, J. Am. Coll. Cardiol. 59 (2012) 1337–1349, https://doi.org/10.1016/j.jacc.2011.10.903.

[8] B. Fereidoonnezhad, R. Naghdabadi, S. Sohrabpour, G.A. Holzapfel, A Mechanobiological model for damage-induced growth in arterial tissue with application to in-stent restenosis, J. Mech. Phys. Solid. 101 (2017) 311–327, https://doi.org/10.1016/j.jmps.2017.01.016.

[9] C. Souilhol, J. Serbanovic-Canic, M. Fragiadaki, T.J. Chico, V. Ridger, H. Roddie, P.C. Evans, Endothelial responses to shear stress in atherosclerosis: a novel role for developmental genes, Nat. Rev. Cardiol. 17 (2020) 52–63, https://doi.org/10.1038/s41569-019-0239-5.

[10] M. Ezzati, A.D. Lopez, A. Rodgers, S. Vander Hoorn, C.J.L. Murray, Comparative Risk Assessment Collaborating Group, Selected major risk factors and global and regional burden of disease, Lancet 360 (2002) 1347–1360, https://doi.org/10.1016/S0140-6736(02)11403-6.

[11] V. Prystopiuk, B. Fels, C.S. Simon, I. Liashkovich, D. Pasrednik, C. Kronlage, R. Wedlich-Söldner, H. Oberleithner, J. Fels, A two-phase response of endothelial cells to hydrostatic pressure, J. Cell Sci. 131 (2018), https://doi.org/10.1242/jcs.206920 jcs206920.

[12] J.J. O'Donnell, A.A. Birukova, E.C. Beyer, K.G. Birukov, Gap junction protein connexin43 exacerbates lung vascular permeability, PLoS One 9 (2014), e100931, https://doi.org/10.1371/journal.pone.0100931.

[13] H. Chiba, M. Osanai, M. Murata, T. Kojima, N. Sawada, Transmembrane proteins of tight junctions, Biochim. Biophys. Acta 1778 (2008) 588–600, https://doi.org/10.1016/j.bbamem.2007.08.017.

[14] M. Furuse, Molecular basis of the core structure of tight junctions, Cold Spring Harbor Perspect. Biol. 2 (2010) a002907, https://doi.org/10.1101/cshperspect.a002907.

[15] X. Cong, W. Kong, Endothelial tight junctions and their regulatory signaling pathways in vascular homeostasis and disease, Cell. Signal. 66 (2020), https://doi.org/10.1016/j.cellsig.2019.109485, 109485.

[16] C. Zihni, C. Mills, K. Matter, M.S. Balda, Tight junctions: from simple barriers to multifunctional molecular gates, Nat. Rev. Mol. Cell Biol. 17 (2016) 564–580, https://doi.org/10.1038/nrm.2016.80.

[17] L. Shen, C.R. Weber, D.R. Raleigh, D. Yu, J.R. Turner, Tight junction pore and leak pathways: a dynamic duo, Annu. Rev. Physiol. 73 (2011) 283–309, https://doi.org/10.1146/annurev-physiol-012110-142150.

[18] C.M. Van Itallie, A.S. Fanning, A. Bridges, J.M. Anderson, ZO-1 stabilizes the tight junction solute barrier through coupling to the perijunctional cytoskeleton, Mol. Biol. Cell 20 (2009) 3930–3940, https://doi.org/10.1091/mbc.e09-04-0320.

[19] A.S. Fanning, J.M. Anderson, Zonula occludens-1 and -2 are cytosolic scaffolds that regulate the assembly of cellular junctions, Ann. N. Y. Acad. Sci. 1165 (2009) 113–120, https://doi.org/10.1111/j.1749-6632.2009.04440.x.

[20] W.-T. Kuo, L. Zuo, M.A. Odenwald, S. Madha, G. Singh, C.B. Gurniak, C. Abraham, J.R. Turner, The tight junction protein ZO-1 is dispensable for barrier function but critical for effective mucosal repair, Gastroenterology 161 (2021), https://doi.org/10.1053/j.gastro.2021.08.047, 1924–1939.

[21] J. Xu, S.B.H. Lim, M.Y. Ng, S.M. Ali, J.P. Kausalya, V. Limviphuvadh, S. Maurer-Stroh, W. Hunziker, ZO-1 regulates Erk, Smad1/5/8, Smad2, and RhoA activities to modulate self-renewal and differentiation of mouse embryonic stem cells, Stem Cell. 30 (2012) 1885, https://doi.org/10.1002/stem.1172. –1900.

[22] C. Schwayer, S. Shamipour, K. Pranjic-Ferscha, A. Schauer, M. Balda, M. Tada, K. Matter, C.-P. Heisenberg, Mechanosensation of tight junctions depends on ZO-1 phase separation and flow, Cell 179 (2019) 937–952, https://doi.org/10.1016/j.cell.2019.10.006, e18.

[23] T. Katsuno, K. Umeda, T. Matsui, M. Hata, A. Tamura, M. Itoh, K. Takeuchi, T. Fujimori, Y. Nabeshima, T. Noda, S. Tsukita, S. Tsukita, Deficiency of zonula occludens-1 causes embryonic lethal phenotype Associated with defected Yolk sac Angiogenesis and apoptosis of embryonic cells, MBoC 19 (2008) 2465–2475, https://doi.org/10.1091/mbc.e07-12-1215.

[24] J. Zhang, K.P. Vincent, A.K. Peter, M. Klos, H. Cheng, S.M. Huang, J.K. Towne, D. Ferng, Y. Gu, N.D. Dalton, Y. Chan, R. Li, K.L. Peterson, J. Chen, A.D. McCulloch, K.U. Knowlton, R.S. Ross, Cardiomyocyte expression of ZO-1 is essential for normal Atrioventricular conduction but does not alter ventricular function, Circ. Res. 127 (2020) 284–297, https://doi.org/10.1161/CIRCRESAHA.119.315539.

[25] J. Rossa, C. Ploeger, F. Vorreiter, T. Saleh, J. Protze, D. Günzel, H. Wolburg, G. Krause, J. Piontek, Claudin-3 and claudin-5 protein folding and assembly into the tight junction are controlled by non-conserved residues in the transmembrane 3 (TM3) and extracellular loop 2 (ECL2) segments, J. Biol. Chem. 289 (2014) 7641–7653, https://doi.org/10.1074/jbc.M113.531012.

[26] R. Rao, Occludin phosphorylation in regulation of epithelial tight junctions, Ann. N. Y. Acad. Sci. 1165 (2009) 62–68, https://doi.org/10.1111/j.1749-6632.2009.04054.x.

[27] S.M. Krug, S. Amasheh, J.F. Richter, S. Milatz, D. Günzel, J.K. Westphal, O. Huber, J.D. Schulzke, M. Fromm, Tricellulin forms a barrier to macromolecules in tricellular tight junctions without affecting ion permeability, Mol. Biol. Cell 20 (2009) 3713–3724, https://doi.org/10.1091/mbc.e09-01-0080.

[28] S. Lohmann, C. Giampietro, F.M. Pramotton, D. Al-Nuaimi, A. Poli, P. Maiuri, D. Poulikakos, A. Ferrari, The role of Tricellulin in epithelial jamming and Unjamming via segmentation of tricellular junctions, Adv. Sci. 7 (2020), 2001213, https://doi.org/10.1002/advs.202001213.

[29] A.J. Haas, C. Zihni, A. Ruppel, C. Hartmann, K. Ebnet, M. Tada, M.S. Balda, K. Matter, Interplay between extracellular matrix stiffness and JAM-A regulates mechanical load on ZO-1 and tight junction assembly, Cell Rep. 32 (2020), 107924, https://doi.org/10.1016/j.celrep.2020.107924.

[30] K. Zhang, Y. Chen, T. Zhang, L. Huang, Y. Wang, T. Yin, J. Qiu, H. Gregersen, G. Wang, A novel role of Id1 in regulating oscillatory shear stress-mediated lipid Uptake in endothelial cells, Ann. Biomed. Eng. 46 (2018) 849–863, https://doi.org/10.1007/s10439-018-2000-3.

[31] J. Zhao, Z. Mo, F. Guo, D. Shi, Q.Q. Han, Q. Liu, Drug loaded nanoparticle coating on totally bioresorbable PLLA stents to prevent in-stent restenosis, J. Biomed. Mater. Res. B Appl. Biomater. 106 (2018) 88–95, https://doi.org/10.1002/jbm.b.33794.

[32] T. Yin, R. Du, Y. Wang, J. Huang, S. Ge, Y. Huang, Y. Tan, Q. Liu, Z. Chen, H. Feng, J. Du, Y. Wang, G. Wang, Two-stage degradation and novel functional endothelium characteristics of a 3-D printed bioresorbable scaffold, Bioact. Mater. 10 (2022) 378–396, https://doi.org/10.1016/j.bioactmat.2021.08.020.

[33] H. Bauer, J. Zweimueller-Mayer, P. Steinbacher, A. Lametschwandtner, H.C. Bauer, The dual role of zonula occludens (ZO) proteins, J. Biomed. Biotechnol. 2010 (2010), 402593, https://doi.org/10.1155/2010/402593.

[34] T. Otani, M. Furuse, Tight junction structure and function revisited, Trends Cell Biol. 30 (2020) 805–817, https://doi.org/10.1016/j.tcb.2020.08.004.

[35] K.D. Rochfort, P.M. Cummins, Cytokine-mediated dysregulation of zonula occludens-1 properties in human brain microvascular endothelium, Microvasc. Res. 100 (2015) 48–53, https://doi.org/10.1016/j.mvr.2015.04.010.

[36] W. Chen, X.-Z. Ju, Y. Lu, X.-W. Ding, C.-H. Miao, J.-W. Chen, Propofol improved hypoxia-impaired integrity of blood-brain barrier via modulating the expression and phosphorylation of zonula occludens-1, CNS Neurosci. Ther. 25 (2019) 704–713, https://doi.org/10.1111/cns.13101.

[37] S. Lin, P. Dong, C. Zhou, L.A.P. Dallan, V.N. Zimin, G.T.R. Pereira, J. Lee, Y. Gharaibeh, D.L. Wilson, H.G. Bezerra, L. Gu, Degradation modeling of poly-l-lactide acid (PLLA) bioresorbable vascular scaffold within a coronary artery, Nanotechnol. Rev. 9 (2020) 1217–1226, https://doi.org/10.1515/ntrev-2020-0093.

[38] X. Chen, X. Wu, Z. Fan, Q. Zhao, Q. Liu, Biodegradable poly(trimethylene carbonate- *b* -(*L* -lactide- *ran* -glycolide)) terpolymers with tailored molecular structure and advanced performance, Polym. Adv. Technol. 29 (2018) 1684–1696, https://doi.org/10.1002/pat.4272.

[39] H. Tamai, K. Igaki, E. Kyo, K. Kosuga, A. Kawashima, S. Matsui, H. Komori, T. Tsuji, S. Motohara, H. Uehata, Initial and 6-month results of biodegradable poly-l-lactic acid coronary stents in humans, Circulation 102 (2000) 399–404, https://doi.org/10.1161/01.cir.102.4.399.

[40] S. Nishio, K. Kosuga, K. Igaki, M. Okada, E. Kyo, T. Tsuji, E. Takeuchi, Y. Inuzuka, S. Takeda, T. Hata, Y. Takeuchi, Y. Kawada, T. Harita, J. Seki, S. Akamatsu, S. Hasegawa, N. Bruining, S. Brugaletta, S. de Winter, T. Muramatsu, Y. Onuma, P.W. Serruys, S. Ikeguchi, Long-Term (>10 Years) clinical outcomes of first-in-human biodegradable poly-l-lactic acid coronary stents: igaki-Tamai stents, Circulation 125 (2012) 2343–2353, https://doi.org/10.1161/CIRCULATIONAHA.110.000901.

[41] Y. Onuma, P.W. Serruys, L.E.L. Perkins, T. Okamura, N. Gonzalo, H.M. García-García, E. Regar, M. Kamberi, J.C. Powers, R. Rapoza, H. van Beusekom, W. van der Giessen, R. Virmani, Intracoronary optical coherence tomography and histology at 1 Month and 2, 3, and 4 Years after implantation of everolimus-eluting bioresorbable vascular scaffolds in a porcine coronary artery model, Circulation 122 (2010) 2288–2300, https://doi.org/10.1161/CIRCULATIONAHA.109.921528.

[42] O. Beutel, R. Maraspini, K. Pombo-García, C. Martin-Lemaitre, A. Honigmann, Phase separation of zonula occludens proteins drives formation of tight junctions, Cell 179 (2019) 923–936, https://doi.org/10.1016/j.cell.2019.10.011, e11.